Transformation of GaAs into an indirect *L*-band-gap semiconductor under uniaxial strain

P. Grivickas, M. D. McCluskey, and Y. M. Gupta
Department of Physics and Astronomy and Institute for Shock Physics, Washington State University, Pullman, Washington 99164-2816, USA
(Received 4 June 2009; published 5 August 2009)

We report the direct-to-indirect band-gap transition in GaAs under nonhydrostatic compression. Uniaxial strain was produced in GaAs single crystals by impact loading along the [100] and [111] orientations up to longitudinal stresses of 5.5 GPa. Band-gap shifts were determined from low-temperature photoluminescence measurements from Te- and Zn-doped samples. For strain along the [100] direction, GaAs undergoes a Γ-*X* band transition similar to what occurs under hydrostatic pressure. Strain along [111], in contrast, produces a large splitting of the *L* band. This causes the *L*-band minimum to plunge downward and transform GaAs into an indirect *L*-band-gap semiconductor.

DOI: 10.1103/PhysRevB.80.073201 PACS number(s): 71.70.Fk, 62.50.−p, 71.55.Eq, 78.55.Cr

The effect of strains on the band structure of semiconductors is of fundamental interest in condensed-matter physics. Intervalley scattering processes involving electronic transitions between different conduction-band (CB) minima depend strongly on the deformation potentials.[1,2] In strained semiconductors, band-gap distortions affect carrier transport and recombination processes.[3,4] Strain effects are particularly important as dimensions approach the nanoscale; strains can reach 3% in quantum-well heterostructures[5] and up to 7% in quantum dots,[6] resulting in significant changes in the optical properties.

Semiconductors with the diamond or zinc-blende crystal structure have CB minima located at the [000] (Γ), [100] (*X*), and [111] (*L*) symmetry points of the Brillouin zone.[7] Under hydrostatic pressure, the CB minima at the Γ and *L* points shift upward in energy, with the shift being larger for the Γ band while the *X*-band minimum shifts downward.[8] These shifts alter the band gap of each semiconductor in a unique way. Si shows a constant reduction in the indirect *X* band gap with applied pressure.[9] In Ge, an initial gradual increase in the indirect *L* band gap intersects the decreasing indirect *X* band gap at 3.5 GPa.[10]

Most III–V compound semiconductors have a direct Γ band gap at ambient conditions. Under hydrostatic pressure, the upward shift of the Γ band eventually intersects the *X* band and the material undergoes a direct-to-indirect transition (DIT).[11,12] In GaAs, the DIT was observed at ~4 GPa by measuring absorption[13,14] and photoluminescence (PL) (Refs. 15 and 16) spectra in diamond-anvil cells. Due to the technological importance of GaAs, the DIT was used to investigate various aspects of band-structure theory including the scattering cross sections of intraband transitions,[1,2] the formation of shallow impurities,[17–19] the nature and origin of the DX center,[20–22] and the dynamics of excited carriers.[23,24]

Application of hydrostatic pressure to a cubic crystal causes the volume to decrease while preserving the crystal symmetry. In contrast, an arbitrary strain tensor, e_{ij}, can always be decomposed into a spherical part (volumetric strains) and a deviatoric part (shear strains). The deviatoric strains alter the symmetry and lift the degeneracy of electronic states. The role of deviatoric strains can be studied by applying uniaxial stress loading along different crystallographic orientations. In GaAs, however, DIT due to deviatoric strains has never been observed because of brittle failure at uniaxial stresses exceeding 1 GPa.[25] In the present work, we overcame this difficulty by applying uniaxial strain loading along the [100] and [111] orientations of GaAs to achieve longitudinal stresses up to 5.5 GPa. The large deviatoric strains produced in these experiments caused the DIT.

The experimental configuration is shown schematically in the inset of Fig. 1. Samples, cut from the [100]- and [111]-oriented GaAs wafers, were sandwiched between the buffer and optical window materials using springs. The target was mechanically attached to an aluminum holder and cooled by liquid nitrogen. Uniaxial strain compression was produced by impacting the front surface of the buffer material with a known impactor mounted on a projectile accelerated to the desired impact velocity. The particular loading condition at the probed sample surface depended on the choice of the buffer material preceding the sample. *Z*-cut quartz[26] resulted in a near-discontinuous jump followed by a constant longitudinal stress for ~200 ns. Fused silica[27] resulted in a continuous increase in longitudinal stress up to 5.5 GPa over a duration of ~150 ns. The exact time evolution of the compression loading profiles was obtained from the particle velocity history measured using velocity interferometer system for any reflector (VISAR).[28,29] The longitudinal stress was

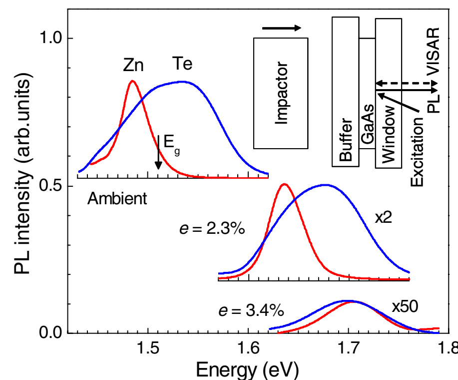

FIG. 1. (Color online) PL peaks of GaAs:Zn and GaAs:Te at different uniaxial strains in discontinuous-compression experiments. Inset: schematic view of PL measurements in dynamic compression experiments.

 ©2009 The American Physical Society

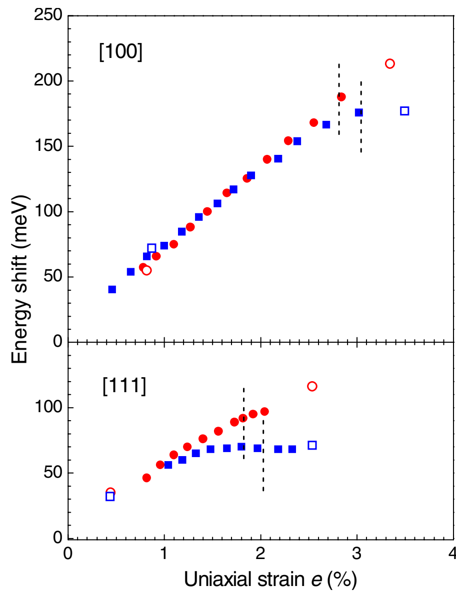

FIG. 2. (Color online) Shift of PL peaks for uniaxial strain along [100] and [111] orientations for discontinuous jumps (open symbols) or continuous increase (solid symbols) in the longitudinal stress. Zn peaks are shown as circles and Te peaks are shown as squares. Dashed lines show the threshold uniaxial strains for which an abrupt loss in PL intensity was observed.

determined from the particle velocity history using the known loading response for the c-axis sapphire windows.[30] The uniaxial strain, e, for different crystallographic orientations was calculated from the longitudinal stress using the low-temperature second-order elastic constants[31] and the room-temperature third-order elastic constants[32] of GaAs. In this work, positive values of e refer to compressive strains.

It was shown previously that the band-structure evolution in GaAs under hydrostatic pressure can be inferred from the shift and intensity changes in Zn-acceptor- and Te-donor-related PL peaks.[16] In the present work, the same information was obtained from continuous PL collection during dynamic compression. PL was excited using a 514.5 nm, 2 μs dye laser pulse focused onto the center of the sample surface near the GaAs-window interface. The collected PL was spectrally and temporally dispersed, and recorded using a charge-coupled device detector. Details regarding the analysis of the intensity-wavelength-time data sets in dynamic compression experiments can be found in Refs. 33 and 34.

Figure 1 shows ambient PL spectra for Te- and Zn-doped ($\sim 10^{18}$ cm^{-3}) GaAs samples. The shape of the ambient peaks near the 1.51 eV band gap was consistent with the band-to-impurity recombination observed at low temperatures.[35] During discontinuous compression to $e=2.3\%$ along the [100] orientation, both PL peaks shifted to higher energies and showed some loss of PL intensity. At $e=3.4\%$, the shifts increased but the PL intensities decreased by more than an order of magnitude (all peaks were smoothed using a fast Fourier transform filter).

The shifts of both PL peaks during discontinuous or shock wave compression are shown as open symbols in Fig. 2. Data gaps between discontinuous strain compression values were filled using PL shifts observed under continuous compression, shown as solid symbols in Fig. 2. The two compression methods showed good agreement. For both orientations, an increasing separation between Zn (circles) and Te (squares) peaks occurred at large uniaxial strains.

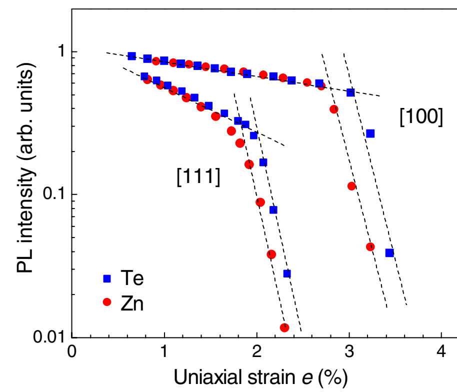

FIG. 3. (Color online) Change in the integrated PL peak intensity for continuous increase in compression along [100] and [111] orientations. Zn peaks are shown as circles and Te peaks are shown as squares. Distinct regions in the intensity dependence are identified using dashed lines.

Continuous compression was also used to follow the integrated PL peak intensity changes. Figure 3 shows that an abrupt PL intensity loss occurred at a particular uniaxial strain value for each orientation. These transition values were similar for both Zn acceptors and Te donors. The intersections between the two distinct regions in the intensity dependence (dashed lines in Fig. 3) were labeled as the "threshold" uniaxial strains. They are identified by the vertical dashed lines in Fig. 2.

The PL changes under uniaxial strain are similar to those observed for DIT under hydrostatic pressure.[16] The initial blueshift of the PL peaks follows the increase in the Γ minimum. The subsequent abrupt loss in PL intensity occurs due to the transfer of photogenerated electrons from the direct to the indirect minimum at the Γ-X crossover. The difference between the Zn and Te PL peak shifts near the transition arises from the different Fermi-level positions for acceptors and donors. The gradual decrease in PL intensity before the DIT may occur due to density-of-state and effective-mass changes in the split bands.

The uniaxial strain threshold for the DIT was significantly lower for [111] than for the [100] orientation. This finding is opposite to what one would expect from the symmetry of the X band[36] for the following reasons. The deviatoric strains due to uniaxial strain compression along [100] split the X band into two components but not for compression along [111]. The splitting for compression along [100] causes the X-band minimum to decrease more rapidly along this orientation. Hence, the Γ-X crossover should occur at a *lower* strain for [100], contrary to what is observed experimentally.

To understand our results, the role of the L band[36] has been considered. This band, unlike the X band, splits into two components for compression along [111] but not for compression along [100]. The splitting for compression along [111] causes the L-band minimum to decrease more rapidly along this orientation, in agreement with our findings.

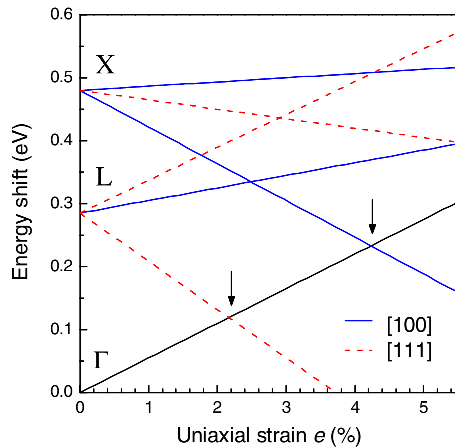

FIG. 4. (Color online) Evolution of three conduction-band minima in GaAs for uniaxial strain along [100] (solid lines) and [111] (dashed lines) orientations.

The shear deformation potentials for the X and L bands were estimated from hot PL measurements of uniaxially stressed GaAs.[37] Using these parameters, together with the hydrostatic deformation potentials and band gaps of GaAs,[38] we modeled the evolution of the CBs under uniaxial strain (Fig. 4). Our calculations show that for uniaxial strain along the [100] orientation, the first band to cross the Γ band (at $e=4.2\%$) is the lowest component of the X band. For uniaxial strain along the [111] orientation, the first band to cross the Γ band (at $e=2.2\%$) is the lowest component of the L band. These crossover points are indicated by the arrows in Fig. 4. The calculated values are close to the experimentally observed DIT points at $e=3\%$ and 2% for [100] and [111] orientations, respectively (Fig. 3). These results support the conclusion that the X band is responsible for the transition under [100] strain, whereas the L band is responsible for the transition under [111] strain.

In conclusion, we have observed the direct-to-indirect band-gap transition in GaAs under nonhydrostatic compression. Unlike the hydrostatic pressure results, where the DIT occurs between the X and Γ bands, the nature of the transition under uniaxial strain compression is strongly anisotropic and depends on the crystallographic orientation. These findings are important for determining the influence of the L band on transport phenomena in GaAs. Our experiments also provide an approach to study the electronic properties of GaAs nanostructures, where significant nonhydrostatic deformations can exist due to surface and interface strains.[39]

This work was supported by DOE under Grant No. DE-FG03-97SF21388. M.D.M. acknowledges partial support by NSF.

[1] A. R. Goñi, A. Cantarero, K. Syassen, and M. Cardona, Phys. Rev. B **41**, 10111 (1990).
[2] J. Sjakste, V. Tyuterev, and N. Vast, Phys. Rev. B **74**, 235216 (2006).
[3] M. V. Fischetti and S. E. Laux, J. Appl. Phys. **80**, 2234 (1996).
[4] Y. Sun, S. E. Thompson, and T. Nishida, J. Appl. Phys. **101**, 104503 (2007).
[5] B. M. Arora, K. S. Chandrasekaran, M. R. Gokhale, G. Nair, G. V. Rao, G. Amarendra, and B. Viswanathan, J. Appl. Phys. **87**, 8444 (2000).
[6] G. Bester, A. Zunger, X. Wu, and D. Vanderbilt, Phys. Rev. B **74**, 081305(R) (2006).
[7] P. Y. Yu and M. Cardona, *Fundamentals of Semiconductors, Physics and Materials Properties* (Springer, New York, 2001).
[8] T. Suski and W. Paul, *High Pressure in Semiconductor Physics I and II*, Semiconductors and Semimetals Vols. 54 and 55 (Academic Press, London, 1998).
[9] B. Welber, C. K. Kim, M. Cardona, and S. Rodriguez, Solid State Commun. **17**, 1021 (1975).
[10] A. Jayaraman, B. B. Kosicki, and J. C. Irvin, Phys. Rev. **171**, 836 (1968).
[11] A. L. Edwards and H. G. Drickamer, Phys. Rev. **122**, 1149 (1961).
[12] H. Muller, R. Trommer, M. Cardona, and P. Vogl, Phys. Rev. B **21**, 4879 (1980).
[13] B. Welber, M. Cardona, C. K. Kim, and S. Rodriguez, Phys. Rev. B **12**, 5729 (1975).
[14] A. R. Goni, K. Strossner, K. Syassen, and M. Cardona, Phys. Rev. B **36**, 1581 (1987).
[15] P. Y. Yu and B. Welber, Solid State Commun. **25**, 209 (1978).
[16] D. Olego, M. Cardona, and H. Muller, Phys. Rev. B **22**, 894 (1980).
[17] D. J. Wolford and J. A. Bradley, Solid State Commun. **53**, 1069 (1985).
[18] A. Kangarlu, H. Guarriello, R. Berney, and P. W. Yu, Appl. Phys. Lett. **59**, 2290 (1991).
[19] L. Hsu, S. Zehender, E. Bauser, and E. E. Haller, Phys. Rev. B **55**, 10515 (1997).
[20] X. Liu, L. Samuelson, M.-E. Pistol, M. Gerling, and S. Nilsson, Phys. Rev. B **42**, 11791 (1990).
[21] M. Holtz, T. Sauncy, T. Dallas, and S. Massie, Phys. Rev. B **50**, 14706 (1994).
[22] J. Zeman, M. Zigone, and G. Martinez, Phys. Rev. B **51**, 17551 (1995).
[23] M. Leroux, G. Pelous, F. Raymond, and C. Verie, Appl. Phys. Lett. **46**, 288 (1985).
[24] H. Mariette, D. J. Wolford, and J. A. Bradley, Phys. Rev. B **33**, 8373 (1986).
[25] M. Cardona, Phys. Status Solidi B **198**, 5 (1996).
[26] S. C. Jones and Y. M. Gupta, J. Appl. Phys. **88**, 5671 (2000).
[27] L. M. Barker and R. E. Hollenbach, J. Appl. Phys. **41**, 4208 (1970).
[28] L. M. Barker and R. E. Hollenbach, J. Appl. Phys. **43**, 4669 (1972).
[29] L. M. Barker and K. W. Schuler, J. Appl. Phys. **45**, 3692 (1974).
[30] S. C. Jones, M. C. Robinson, and Y. M. Gupta, J. Appl. Phys. **93**, 1023 (2003).
[31] R. I. Cottam and G. A. Saunders, J. Phys. C **6**, 2105 (1973).

[32] A. S. Johal and D. J. Dunstan, Phys. Rev. B **73**, 024106 (2006).
[33] X. A. Shen and Y. M. Gupta, Phys. Rev. B **48**, 2929 (1993).
[34] P. Grivickas, M. D. McCluskey, and Y. M. Gupta, Phys. Rev. B **75**, 235207 (2007).
[35] J. I. Pankove, *Optical Processes in Semiconductors* (Prentice-Hall, New Jersey, 1971).
[36] I. Balslev, Phys. Rev. **143**, 636 (1966).
[37] D. N. Mirlin, V. F. Sapega, I. Ya. Karlik, and R. Katilius, Solid State Commun. **61**, 799 (1987).
[38] S. Adachi, *GaAs and Related Materials, Bulk Semiconducting and Superlattice Properties* (World Scientific, New Jersey, 1994).
[39] Q. Shen, S. W. Kycia, E. S. Tentarelli, W. J. Schaff, and L. F. Eastman, Phys. Rev. B **54**, 16381 (1996).